

5C) (20). The constitutive kinase activation of all KIT mutants found in the five GISTs was confirmed in Ba/F3 cells (Fig. 5D) (5, 21).

Although various cells including hematopoietic stem cells express both KIT and CD34 (22), ICCs are the only cells that are double-positive for KIT and CD34 in normal GI wall of humans. This strongly suggests that KIT and CD34 double-positive GISTs might originate from ICCs, although we cannot exclude the possibility that ICCs and GISTs simply show common undifferentiated characteristics such as those observed in multipotential hematopoietic stem cells.

The mechanism by which KIT becomes constitutively activated appears to be different for the tyrosine kinase domain mutant and the juxtamembrane domain mutant (6, 21). The former is constitutively activated without forming dimers (21), whereas the latter constitutively dimerizes without binding SCF (6, 21). The tyrosine kinase domain mutation of KIT has been found only in mast cell neoplasms (7) and its juxtamembrane domain mutation only in GISTs. The mechanisms by which these different mutations cause malignant transformation of different cell types remain to be investigated.

REFERENCES AND NOTES

1. P. Besmer *et al.*, *Nature* **320**, 415 (1986); B. Chabot, D. A. Stephenson, V. M. Chapman, P. Besmer, A. Bernstein, *ibid.* **335**, 88 (1988); E. N. Geissler, M. A. Ryan, D. E. Houseman, *Cell* **55**, 185 (1988).
2. D. E. Williams *et al.*, *Cell* **63**, 167 (1990); J. G. Flanagan and P. Leder, *ibid.*, p. 185; K. M. Zsebo *et al.*, *ibid.*, p. 213; E. Huang *et al.*, *ibid.*, p. 225.
3. E. S. Russel, *Adv. Genet.* **20**, 357 (1979); Y. Kitamura, S. Go, K. Hatanaka, *Blood* **52**, 447 (1978); Y. Kitamura and S. Go, *ibid.* **53**, 492 (1979).
4. H. Maeda *et al.*, *Development* **116**, 369 (1992); J. D. Huizinga *et al.*, *Nature* **373**, 347 (1995); K. Isozaki *et al.*, *Gastroenterology* **109**, 456 (1995).
5. T. Furitsu *et al.*, *J. Clin. Invest.* **92**, 1736 (1993).
6. T. Tsujimura *et al.*, *Blood* **83**, 2619 (1994); T. Tsujimura *et al.*, *Int. Arch. Allergy Immunol.* **106**, 377 (1995); T. Tsujimura *et al.*, *Blood* **87**, 273 (1996).
7. H. Nagata *et al.*, *Proc. Natl. Acad. Sci. U.S.A.* **92**, 10560 (1995); B. J. Longley *et al.*, *Nature Genet.* **12**, 312 (1996).
8. Formalin-fixed paraffin sections (3 μ m thick) were used (23). For enzyme immunohistochemistry, rabbit polyclonal antibody against human KIT (K963; IBL, Fujioka, Japan) and mouse monoclonal antibody (mAb) against human CD34 (QBend10; Novocastra laboratories, Newcastle, UK) were used as the primary antibodies. Biotinylated goat antibody to rabbit (anti-rabbit) immunoglobulin G (IgG) and biotinylated rabbit anti-mouse IgG (DAKO; Glostrup, Denmark) were used as the secondary antibodies. Binding of the secondary antibodies was visualized as in (23). Coexpression of KIT and CD34 was confirmed with a confocal laser scanning microscope (Olympus LSM-GB200; Olympus, Tokyo, Japan). Fluorescein isothiocyanate (FITC)-conjugated swine anti-rabbit IgG and R-phycoerythrin (RPE)-conjugated goat anti-mouse IgG (DAKO) were used as the secondary antibodies. The excitation wavelength is 488 nm for FITC and 515 nm for RPE.
9. M. van de Rijn, M. R. Hendrickson, R. V. Rouse,

Hum. Pathol. **25**, 776 (1994); J. M. Monihan, N. J. Carr, L. H. Sobin, *Histopathology* **25**, 469 (1994); M. Miettinen, M. Virolainen, M. S. Rikala, *Am. J. Surg. Pathol.* **19**, 207 (1995).

10. M. S. Fausson-Pellegrini, D. Panthalone, C. Cortesini, *J. Submicrosc. Cytol. Pathol.* **21**, 439 (1987); J.-M. Vanderwinden, H. Liu, M.-H. D. Laet, J.-J. Vanderhaeghen, *Gastroenterology* **111**, 279 (1996).
11. R. Matsuda *et al.*, *Am. J. Pathol.* **142**, 339 (1993); J.-M. Vanderwinden *et al.*, *Gastroenterology* **111**, 901 (1996); J. J. Rumessen, H. B. Mikkelsen, L. Thuneberg, *ibid.* **102**, 56 (1992); J. J. Rumessen, H. B. Mikkelsen, K. Qvortrup, L. Thuneberg, *ibid.* **104**, 343 (1993).
12. M. S. Fausson-Pellegrini, C. Cortesini, D. Panthalone, *Can. J. Physiol. Pharmacol.* **68**, 1437 (1990); J. J. Rumessen, S. Peters, L. Thuneberg, *Lab. Invest.* **68**, 481 (1993).
13. From 10 μ g of total RNA, cDNA was synthesized and amplified as in (24). Oligonucleotide primer sets used were as described (5). The cDNAs were sequenced directly or after subcloning into Bluescript I KS(-) by Model 373A DNA sequencer (Applied Biosystems, Foster City, CA).
14. The coding region of the human wild-type *c-kit* was cloned into Xba I site of expression vector pEF-BOS. The *Sna* BI-Mro I fragment (nucleotide 1141 to 2282) of the human wild-type *c-kit* in the expression vector was replaced by the corresponding fragments of the mutant-type cDNA obtained from each GIST. The expression vectors were transfected into the 293T HEK cell line by calcium phosphate precipitation (5).
15. The procedures of cell lysis, immunoprecipitation, SDS-polyacrylamide gel electrophoresis, and immunoblotting were done as in (5). Mouse mAb to human KIT (MCA955; Serotec, Oxford, UK) was used for the immunoprecipitation. Immunoblotting was done with mouse mAb to phosphotyrosine (4G10; Upstate Biotechnology, Lake Placid, NY) or rabbit polyclonal anti-human KIT (K963).
16. The immune complex kinase assay was done as in (5). Rabbit polyclonal anti-human KIT (K963) was used for the immunoprecipitation.
17. To generate the murine-type *c-kit* cDNAs containing

the same mutation as the GISTs, we performed site-directed mutagenesis (5). The Nde I-Spl I fragment with the mutation was isolated and inserted into the expression vector pEF-BOS containing murine wild-type *c-kit* cDNA.

18. A *Sca* I-cut expression vector pEF-BOS containing the mouse-type mutated *c-kit* cDNA and the Bam HI-cut expression vector pSV2-neo were cotransfected into the IL-3-dependent Ba/F3 murine lymphoid cell line with the use of GENE PULSER II (Bio-Rad Laboratories). After transfection, the cells expressing neomycin-resistant gene were selected by cultivation in medium containing G418 (0.6 mg/ml) and rml-3 for 4 weeks. Cloning of the cells was done with the limiting-dilution method, and the expression of each mutated *c-kit* was confirmed by flow cytometry, protein immunoblotting, and RT-PCR with sequencing.
19. To quantitate cell proliferation, we used the MTT [3-(4,5-dimethylthiazol-2-yl)-2,5-diphenyl tetrazolium bromide] (Sigma) rapid colorimetric assay. The procedure was done as in (6).
20. Cells (10⁷) were transplanted subcutaneously at the posterior flank of nude mice. Untransfected Ba/F3 cells and Ba/F3 cells expressing the murine wild-type KIT were used as controls. Tumors were measured with the vernier caliper every 4 days. The tumor volume (V) was calculated with the formula $V = 0.5 \times a \times b^2$, where *a* and *b* are the length and width in millimeters of the tumor mass, respectively.
21. H. Kitayama *et al.*, *Blood* **85**, 790 (1995).
22. L. K. Ashman, A. C. Cambareri, L. B. To, R. J. Levinsky, C. A. Juttner, *ibid.* **78**, 30 (1991); J. P. Catlett, J. A. Leftwich, E. H. Westin, S. Grant, T. F. Huff, *ibid.*, p. 3186.
23. S. Hirota *et al.*, *Lab. Invest.* **72**, 64 (1995).
24. S. Hirota *et al.*, *Arch. Pathol. Lab. Med.* **117**, 996 (1993).
25. We thank A. Fukuyama and K. Morihana for preparing histological sections. Supported by grants from the Japanese Ministry of Education, Science, Culture, and Sports.

13 May 1997; accepted 25 November 1997

Interaction of a Golgi-Associated Kinesin-Like Protein with Rab6

Arnaud Echard, Florence Jollivet, Olivier Martinez, Jean-Jacques Lacapère, Annie Rousselet, Isabelle Janoueix-Lerosey, Bruno Goud*

Rab guanosine triphosphatases regulate vesicular transport and membrane traffic within eukaryotic cells. Here, a kinesin-like protein that interacts with guanosine triphosphate (GTP)-bound forms of Rab6 was identified. This protein, termed Rabkinesin-6, was localized to the Golgi apparatus and shown to play a role in the dynamics of this organelle. The carboxyl-terminal domain of Rabkinesin-6, which contains the Rab6-interacting domain, inhibited the effects of Rab6-GTP on intracellular transport. Thus, a molecular motor is a potential effector of a Rab protein, and coordinated action between members of these two families of proteins could control membrane dynamics and directional vesicular traffic.

Small guanosine triphosphatases (GTPases) of the Rab family play an essential role in the processes that underlie the targeting and fusion of transport vesicles with their appropriate acceptor membrane (1). Within the past few years, several putative effectors that interact with Rab proteins in their GTP-bound conformation have been identified (2). They are not related to each other and appear to

fulfill diverse functions. This finding suggests that Rab proteins have a more complex role than simply regulating the interaction between proteins involved in the recognition of transport vesicles with membranes (3). On the other hand, it is now well established that intracellular organelles and vesicles, including the endoplasmic reticulum (ER) and Golgi membranes, move along cytoskeletal

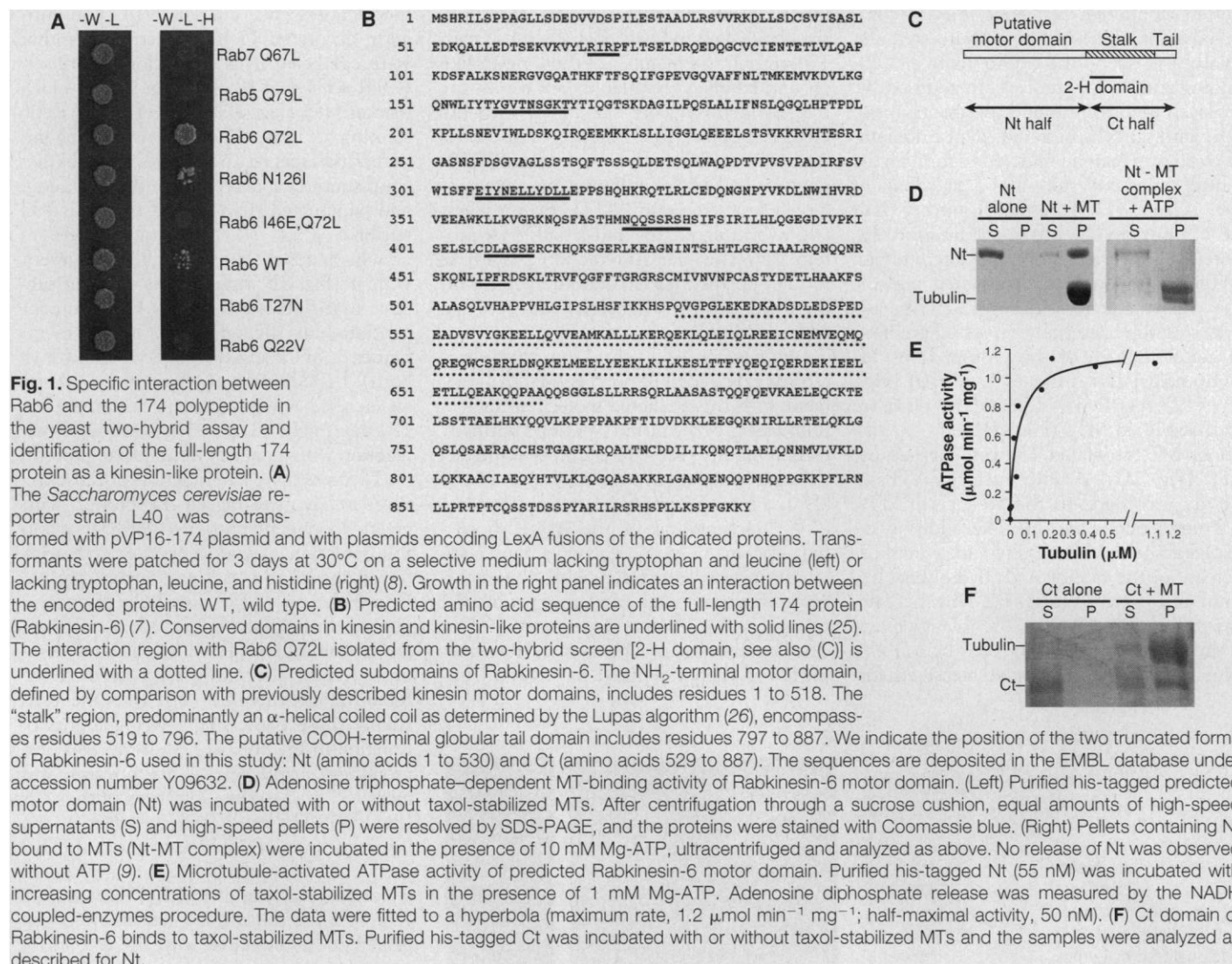


Fig. 1. Specific interaction between Rab6 and the 174 polypeptide in the yeast two-hybrid assay and identification of the full-length 174 protein as a kinesin-like protein. **(A)** The *Saccharomyces cerevisiae* reporter strain L40 was cotransformed with pVP16-174 plasmid and with plasmids encoding LexA fusions of the indicated proteins. Transformants were patched for 3 days at 30°C on a selective medium lacking tryptophan and leucine (left) or lacking tryptophan, leucine, and histidine (right) (8). Growth in the right panel indicates an interaction between the encoded proteins. WT, wild type. **(B)** Predicted amino acid sequence of the full-length 174 protein (Rabkinesin-6) (7). Conserved domains in kinesin and kinesin-like proteins are underlined with solid lines (25). The interaction region with Rab6 Q72L isolated from the two-hybrid screen [2-H domain, see also (C)] is underlined with a dotted line. **(C)** Predicted subdomains of Rabkinesin-6. The NH₂-terminal motor domain, defined by comparison with previously described kinesin motor domains, includes residues 1 to 518. The “stalk” region, predominantly an α -helical coiled coil as determined by the Lupas algorithm (26), encompasses residues 519 to 796. The putative COOH-terminal globular tail domain includes residues 797 to 887. We indicate the position of the two truncated forms of Rabkinesin-6 used in this study: Nt (amino acids 1 to 530) and Ct (amino acids 529 to 887). The sequences are deposited in the EMBL database under accession number Y09632. **(D)** Adenosine triphosphate-dependent MT-binding activity of Rabkinesin-6 motor domain. (Left) Purified his-tagged predicted motor domain (Nt) was incubated with or without taxol-stabilized MTs. After centrifugation through a sucrose cushion, equal amounts of high-speed supernatants (S) and high-speed pellets (P) were resolved by SDS-PAGE, and the proteins were stained with Coomassie blue. (Right) Pellets containing Nt bound to MTs (Nt-MT complex) were incubated in the presence of 10 mM Mg-ATP, ultracentrifuged and analyzed as above. No release of Nt was observed without ATP (9). **(E)** Microtubule-activated ATPase activity of predicted Rabkinesin-6 motor domain. Purified his-tagged Nt (55 nM) was incubated with increasing concentrations of taxol-stabilized MTs in the presence of 1 mM Mg-ATP. Adenosine diphosphate release was measured by the NADH coupled-enzymes procedure. The data were fitted to a hyperbola (maximum rate, 1.2 $\mu\text{mol min}^{-1} \text{mg}^{-1}$; half-maximal activity, 50 nM). **(F)** C-terminal domain of Rabkinesin-6 binds to taxol-stabilized MTs. Purified his-tagged Ct was incubated with or without taxol-stabilized MTs and the samples were analyzed as described for Nt.

elements through an interaction with motor proteins (4, 5). However, the molecular links between the protein machinery involved in the generation and targeting or fusion of transport vesicles and motors are still largely unknown.

Rab6, a ubiquitous Rab associated with Golgi and trans-Golgi network (TGN) membranes, regulates transport within this organelle (6). To identify proteins that interact with the GTP-bound form of Rab6, we used the GTPase-defective mutant Rab6 Gln⁷²→Leu⁷² (Q72L) (7) as bait in a yeast two-hybrid screen of a mouse embryo expression library. Screening of 12 × 10⁶ clones yielded five independent clones that

interacted strongly with Rab6 Q72L, but not with p21ras or lamin, which were used as specificity controls (8). One of them, clone 174, contained a 408-base pair cDNA insert corresponding to an open reading frame (ORF) encoding for a 136-amino acid polypeptide. The 174 polypeptide appeared to be Rab6-specific, because no interaction was detected with Rab5 Gln⁷⁹→Leu⁷⁹ (Q79L) or Rab7 Gln⁶⁷→Leu⁶⁷ (Q67L), which are GTPase-defective mutants of two functionally distinct Rab proteins (Fig. 1A). The 174 polypeptide was found to interact with Rab6 Asn¹²⁶→Ile¹²⁶ (N126I) (a protein expected to be in vivo in its GTP-bound conformation) and, more weakly, with wild-type Rab6 (Fig. 1A). A mutation in the effector domain of Rab6 [Ile⁴⁶→Glu⁴⁶ (I46E), analogous to a mutation that impairs Rab3A activity (3)] abolished the interaction between Rab6 Q72L and the 174 polypeptide (double mutant Rab6 I46E,Q72L) (Fig. 1A). On the

other hand, no interaction was found with the guanosine diphosphate-bound mutants Rab6 Thr²⁷→Asn²⁷ (T27N) and Rab6 Gln²²→Val²² (Q22V). Thus, the 174 polypeptide preferentially interacts with the GTP-bound forms of Rab6, and this interaction is likely to involve the effector domain of Rab6.

Northern (RNA) blot analysis with the 174 cDNA fragment as a probe showed the presence of a predominant 3.6-kb mRNA ubiquitously expressed in various mouse tissue extracts, although at higher amounts in the spleen and testis (9). Using this probe to screen a mouse testis cDNA library, we isolated a clone containing a potential initiator ATG codon, several stop codons in frame upstream of this ATG, and a polyadenylation signal in the 3' noncoding region (10). The predicted protein sequence (Fig. 1B) of this ORF consisted of 887 amino acids and had a calculated relative molecular weight of 99,877. The full-length 174

A. Echard, F. Jollivet, O. Martinez, J.-J. Lacapère, A. Rousselet, B. Goud, Unité Mixte de Recherche CNRS 144 et 168, Institut Curie, 26 rue d'Ulm, 75248 Paris Cedex 05, France.

I. Janoueix-Lerosey, INSERMU 248, Institut Curie, 26 rue d'Ulm, 75248 Paris Cedex 05, France.

*To whom correspondence should be addressed. E-mail: bgoud@curie.fr

protein contained sequence motifs conserved among kinesin-like proteins that are involved in adenosine triphosphate (ATP) binding and ATP hydrolysis. In addition, it displayed a conventional kinesin organization, with an NH₂-terminal motor domain followed by a region predicted to form an α -helical coiled-coil stalk and a tail domain (Fig. 1C) (5, 11). To establish further that the 174 protein belongs to the kinesin-like protein family, we performed microtubule (MT)-binding and MT-activated adenosine triphosphatase (ATPase) activity assays using the bacterially expressed predicted motor domain of the protein (plus 12 amino acids) (Nt, residues 1 to 530) (Fig. 1C) (12). Purified Nt bound *in vitro* to taxol-stabilized MTs (Fig. 1D) (13). In addition, MT-associated Nt was released by ATP (Fig. 1D). A low intrinsic ATPase activity was found in the absence of MTs (6.2 nmol min⁻¹ mg⁻¹). The addition of taxol-stabilized MTs resulted in a marked increase in the rate of ATP hydrolysis (1.2 μ mol min⁻¹ mg⁻¹) (Fig. 1E). This increase corresponded to about a 200-fold increase in the ATPase activity induced by MTs, a value consistent with those measured for

other kinesin-like proteins (5). Altogether, the above data indicate that the full-length 174 protein is a member of the kinesin-like protein family. In available data banks, the highest identity score was found with the CHO1 protein (31% identity and 52.5% similarity over the whole protein and 38.5% identity and 61% similarity over the predicted motor domain) (14). By the yeast two-hybrid assay, the full-length 174 protein gave the same interaction pattern as the 174 polypeptide (9) and interacted with Rab6 *in vivo* (see below). Hence, we termed it Rabkinesin-6.

We next raised an antiserum to the bacterially expressed 174 polypeptide. In agreement with the predicted molecular mass of Rabkinesin-6, the affinity-purified antibody predominantly recognized a protein migrating with an apparent molecular mass of 100 kD in a total lysate of HeLa cells (Fig. 2A) (15). Fractionation of the lysate showed that the major pool of endogenous Rabkinesin-6 was associated with the membrane fraction, even under experimental conditions (4°C) that depolymerize MTs. The localization of endogenous Rabkinesin-6 was then examined by confocal im-

munofluorescence analysis (16). The antibody decorated Golgi-like structures that were colabeled by a monoclonal antibody (CTR 433) that recognizes a medial Golgi marker (17) (Fig. 2B). CTR 433 and Rab6 staining are almost indistinguishable by immunofluorescence (6). However, Rabkinesin-6 staining appeared more discontinuous and punctuated than that of the CTR 433 antibody (Fig. 2B, left) and sometimes closely apposed but not fully congruent with it (Fig. 2B, right). This staining suggests that Rabkinesin-6 may be more concentrated in subdomains of Golgi membranes or in Golgi-associated vesicles (or in both). In addition to Golgi and cytoplasm, we noticed a weak nuclear staining (Fig. 2B) that might be caused by antibody cross-reaction with a nuclear kinesin-like protein.

To investigate the function of Rabkinesin-6 *in vivo*, we tagged the protein with green fluorescent protein (GFP) (to avoid the detection of endogenous protein with the antibody) and transiently overexpressed it in HeLa cells (18). The bulk of overexpressed Rabkinesin-6 (Fig. 3, A and B, green staining) localized to MTs [as demonstrated by costaining with antibody to tubulin (anti-tubulin) (9)]. In some cells (likely those expressing lower amounts of Rabkinesin-6), the MT staining was less prominent, and GFP-Rabkinesin-6 was more localized to the Golgi area of the cells (Fig. 3B). The most striking effect of the overexpression of Rabkinesin-6 was the dispersal of the Golgi apparatus into small structures scattered within the cytoplasm (Fig. 3A, red staining). Such an effect appeared to be correlated with the amount of overexpression of Rabkinesin-6 (compare Fig. 3, A and B). Golgi dispersal was documented with several Golgi and TGN markers, but no marked alteration of the distribution of endosomal and lysosomal compartments was observed (9). In contrast, overexpression of Nt that lacks the stalk region and the COOH-terminus tail, which is thought to be involved in the interaction of kinesin-like proteins with their cargoes (19), did not induce a dispersion of the Golgi apparatus (20) (Fig. 3C). Altogether, the above data suggest a role for Rabkinesin-6 in the dynamics of the Golgi apparatus. Rabkinesin-6 would be expected to be a plus-end-directed motor. The overexpression of Rabkinesin-6 may then increase the concentration of the protein in Golgi membranes and force their movement toward the plus end of MTs, located near the ER and the cell periphery. The microtubular cytoskeleton appeared "bundled" in cells overexpressing Rabkinesin-6. However, we found that the Ct domain of Rabkinesin-6 was able to bind directly *in vitro* and *in vivo* to MTs (12, 13) (Figs. 1F and 3D),

Fig. 2. Endogenous Rabkinesin-6 is a membrane-bound protein and is localized to the Golgi apparatus. **(A)** Total extract, PNS, and proportional amounts of high-speed supernatant (C) and pellet (M) fractions of HeLa cells (15) were analyzed by immunoblotting with rabbit antiserum to Rabkinesin-6 (dilution 1:1000) (top) and anti- β -tubulin (bottom). **(B)** HeLa cells were fixed in methanol and stained with anti-Rabkinesin-6 (dilution 1:2000) (green staining) and a monoclonal antibody to a medial-Golgi antigen (CTR 433) (red staining). The bottom panel shows the superimposition of the two labelings (16). Bars, 10 μ m.

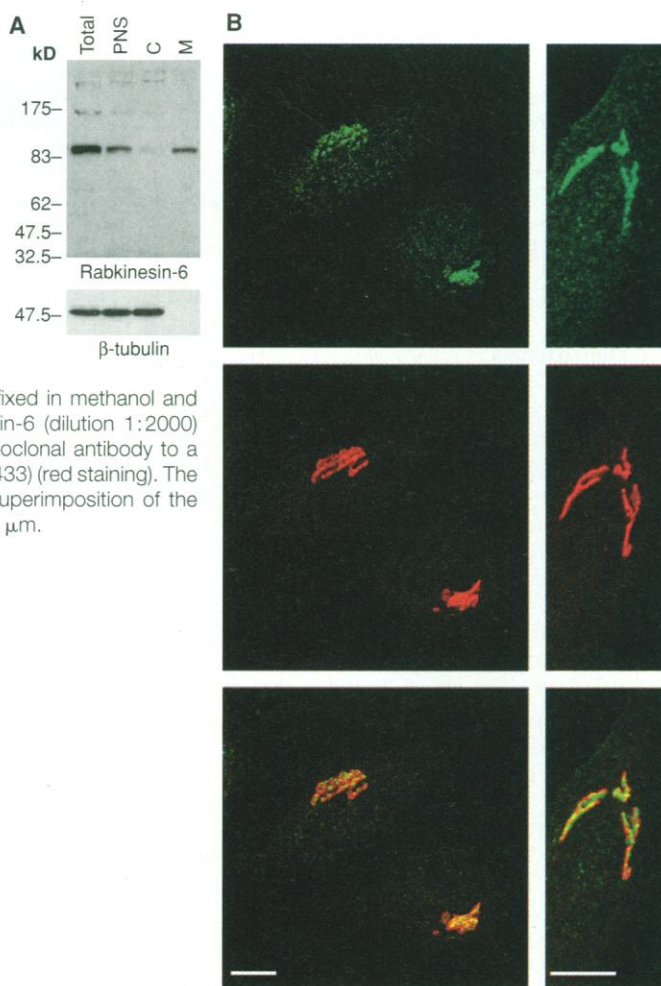


Fig. 3. Effect of the overexpression of GFP-Rabkinesin-6 and Nt or Ct domains of the protein on the morphology of the Golgi apparatus. **(A and B)** Rabkinesin-6 tagged with GFP was transiently expressed in HeLa cells. After 18 hours of transfection, cells were fixed with methanol and stained with CTR 433 antibody to Golgi marker (red staining). In cells expressing high amounts of Rabkinesin-6 **(A)**, the Golgi was dispersed into small structures scattered throughout the cytoplasm. A similar effect was seen with untagged or myc-tagged Rabkinesin-6 or by the overexpression of Rabkinesin-6 with the vaccinia system (6). In cells overexpressing lower amounts of Rabkinesin-6 **(B)**, GFP-Rabkinesin-6 was more localized to the Golgi area, and the Golgi was less dispersed. The right panels in **(A)** and **(B)** show the superimposition of the two labelings. **(C)** Myc-tagged Nt (predicted motor domain) was overexpressed in HeLa cells with the vaccinia system. Nt was revealed with 9E10 anti-myc (red staining), and Golgi (green staining) was decorated with a rabbit antiserum to galactosyltransferase. The figure shows the superimposition of the two labelings. **(D)** Ct (stalk plus tail domain of Rabkinesin-6) was overexpressed in HeLa cells with the vaccinia system. Ct was revealed with the antiserum to Rabkinesin-6 (red staining), and Golgi (green staining) was revealed with the CTR 433 antibody. The figure shows the superimposition of the two labelings. Bars, 10 μ m.

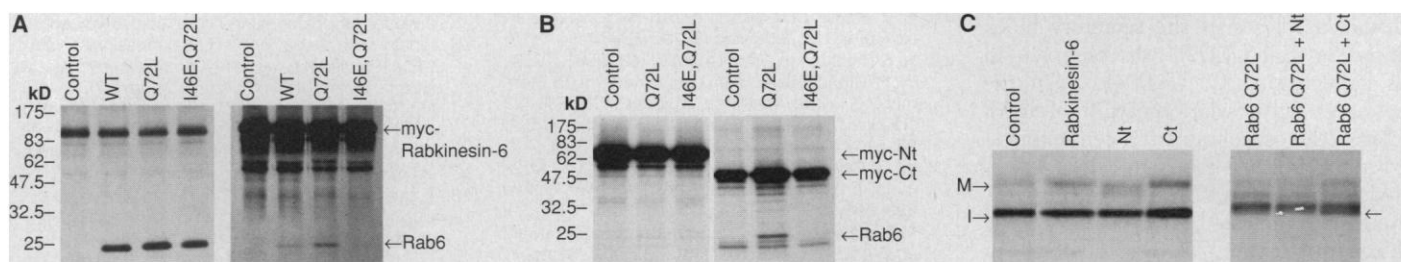
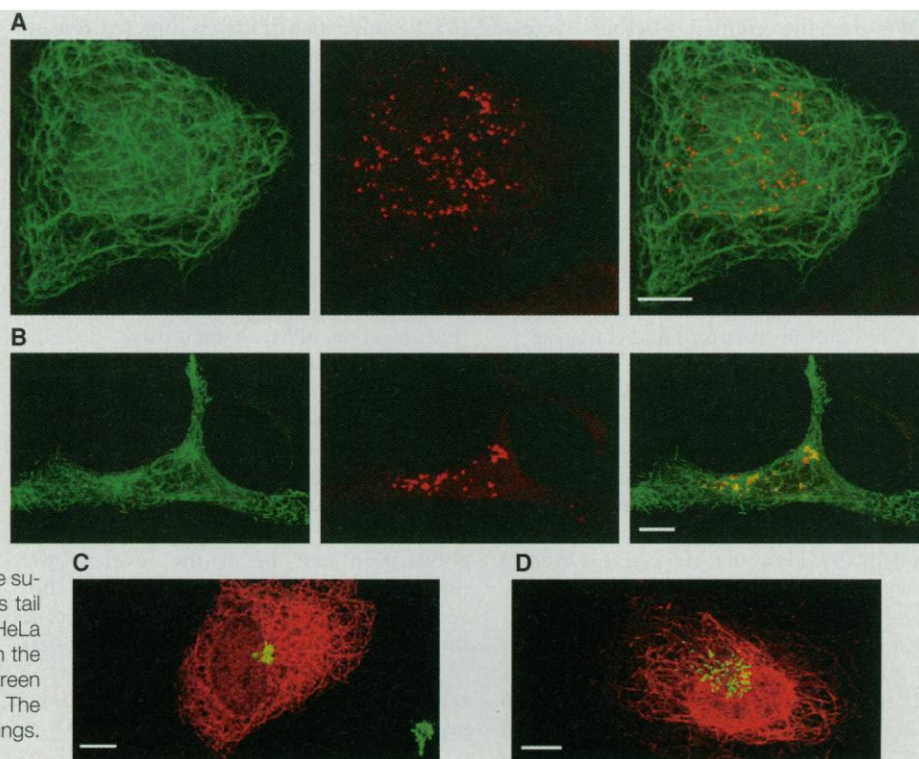


Fig. 4. Rabkinesin-6 and the Ct domain form *in vivo* complexes with Rab6-GTP, and Ct partially reverses the effect of RabQ72L on the transport of SEAP. **(A and B)** HeLa cells were cotransfected with myc-tagged Rabkinesin-6-encoding plasmids **(A)** and myc-tagged Nt- or Ct-encoding plasmids **(B)** and either pGEM-1 (control) or plasmids encoding for Rab6 constructs. After a 20-min metabolic labeling, complexes were immunoprecipitated with 9E10 anti-myc. **(A)** (Left) Cell lysates (1/9 of total) were immunoprecipitated with both anti-Rab6 and anti-myc to determine the amounts of overexpressed Rab6 constructs and Rabkinesin-6 in cell lysates. (Right) Rab6 Q72L and wild-type Rab6, but not Rab6 I46E,Q72L, were immunoprecipitated by anti-myc. The coimmunoprecipitating band was identified as Rab6 by reimmunoprecipitation with anti-Rab6 (9). **(B)** Rab6 Q72L was coimmunoprecipitated with Ct (right) but not with Nt (left). The band migrating under Rab6 in cells expressing Ct likely represents a degradation product of Ct. **(C)** (Left) HeLa cells were cotransfected with SEAP and either the control or Rabkinesin-6-, Nt-, or Ct-encoding plasmids. (Right) HeLa cells were cotransfected with SEAP and either Rab6 Q72L, Rab6 Q72L plus Nt-encoding plasmids, or Rab6 Q72L plus Ct-encoding plasmids. Intracellular SEAP was then immunoprecipitated and analyzed after treatment with endo H by SDS-PAGE and autoradiography (6). M and I represent the mature and immature forms of intracellular SEAP, respectively. The arrow on the right indicates the presence of an immature form of SEAP in cells cotransfected with Ct plus Rab6 Q72L. **(D)** SEAP secreted in media of cells transfected with either pGEM-1 (control), Rab6 Q72L, Rab6 Q72L plus Nt-encoding plasmids, or Rab6 Q72L plus Ct-encoding plasmids was immunoprecipitated and quantified as described above. The results are expressed as the percent of SEAP found in the medium of control cells. Means, \pm SD of three independent experiments.

which suggests that Rabkinesin-6 carries, as conventional kinesin and the kinesin-like protein *ncd* possibly do (21), an MT-binding site outside its motor domain. This finding raises the possibility that Rabkinesin-6 could cross bridge the MTs, explaining such a “bundling” effect.

To investigate the functional relation between Rab6 and Rabkinesin-6, we first demonstrated the direct interaction *in vivo* be-

tween Rab6 and Rabkinesin-6. Myc-tagged Rabkinesin-6 was coexpressed with various Rab6 constructs in HeLa cells (22). Rab6 Q72L and a lower amount of wild-type Rab6 could be immunoprecipitated with anti-myc (Fig. 4A). Conversely, the double mutant Rab6 I46E,Q72L was not coimmunoprecipitated, in good agreement with the data from the two-hybrid assay (Fig. 4A). To further define the interaction between Rab6 and

Rabkinesin-6, we coexpressed Nt or Ct domains of Rabkinesin-6 with Rab6 constructs. Nt did not form complexes with Rab6, which suggests that Rab6 does not interact directly with the motor domain of Rabkinesin-6 (Fig. 4B). On the other hand, Rab6 Q72L was coimmunoprecipitated with Ct (Fig. 4B), consistent with the location of the Rab6-interacting domain identified by the yeast two-hybrid assay.

We then determined whether overexpression of Rabkinesin-6 affects the transport of a secretory marker, such as the secreted form of alkaline phosphatase (SEAP), as does overexpression of Rab6-GTP (6). No marked alteration of the secretory process was observed in HeLa cells overexpressing Rabkinesin-6, Nt, or Ct domains of the protein (23) (Fig. 4C). The two forms of intracellular SEAP, one corresponding to the Golgi-associated, fully glycosylated protein (mature) and the other to immature SEAP still associated with the ER, were detectable in cells overexpressing Rabkinesin-6, Ct, or Nt (although the mature form of SEAP appeared as a doublet in these cells) (Fig. 4C, left). In addition, the release of SEAP in the extracellular medium was comparable with that found in control cells (9). However, the coexpression of Ct with Rab6 Q72L partially reversed the strong effect of Rab6 Q72L on intracellular transport of SEAP (Fig. 4C, right). Whereas the immature form of SEAP was no longer detectable in cells overexpressing Rab6 Q72L [because of the relocalization of Golgi glycosyltransferases into the ER (6)], this form reappeared in cells expressing both Ct and Rab6 Q72L (Fig. 4C, right, arrow). In addition, a release of the secretory block induced by Rab6 Q72L was observed in cells coexpressing Ct (Fig. 4D). On the other hand, a glycosylation pattern of SEAP similar to the one obtained in cells expressing Rab6 Q72L was found in cells cotransfected with Rab6 Q72L and Nt (Fig. 4C, right), and no release of the secretory block induced by Rab6 Q72L was observed in these cells (Fig. 4D). Thus, Ct, which contains the Rabkinesin-6-interacting domain, but not Nt, partially suppressed the Rab6 Q72L effect. A fragmentation of the Golgi could be observed in cells that overexpressed Ct alone (Fig. 3D). A similar effect could be seen in cells overexpressing Rab6 I46E (mutation in the effector domain) (9). One possibility is that the overexpression of Ct alters the function of other Rab6 effectors involved in Golgi dynamics by interfering with their binding to the Rab6 effector domain.

We have previously shown that Rab6-GTP effects, that is, the inhibition of intracellular anterograde transport and the redistribution of Golgi proteins into the ER, require the integrity of MTs (6). A tentative hypothesis is that Rab6 regulates the association and dissociation of Rabkinesin-6 with MTs, which points to a role for Rab6 in the movement of Golgi membranes and their associated vesicles along MTs through an interaction with Rabkinesin-6. This role would be consistent with the proposed role for Rab6 in retrograde membrane traffic at the level of the Golgi apparatus

(6), because such traffic is directed toward the plus end of MTs in this region of the cell. However, the overexpression of Rabkinesin-6 alone was not sufficient to redistribute Golgi resident proteins into the ER, as does the overexpression of Rab6-GTP (6). In addition, the Golgi complex, although dispersed, remained functional in cells overexpressing Rabkinesin-6 (Fig. 4C). A likely interpretation is that, in addition to Rabkinesin-6, Rab6 interacts with other effectors that have yet to be characterized.

Thus, we have identified a kinesin-like protein associated with the Golgi apparatus that interacts with GTP-bound forms of Rab6. A possible link between some GTPases of the Rab family and the cytoskeleton has been documented (24). The present study suggests that this connection may be at the level of the molecular motors. An attractive hypothesis is that Rab proteins (or at least some of them) act in concert with molecular motors to regulate directional membrane transport and dynamics of intracellular organelles.

REFERENCES AND NOTES

1. S. R. Pfeffer, *Curr. Opin. Cell Biol.* **6**, 522 (1994); P. Novick and M. Zerial, *ibid.* **9**, 496 (1997).
2. H. Shirataki *et al.*, *Mol. Cell. Biol.* **13**, 2061 (1993); W. H. Brondyk *et al.*, *ibid.* **15**, 1137 (1995); H. Stenmark, G. Vitale, O. Ullrich, M. Zerial, *Cell* **83**, 423 (1995); M. Ren *et al.*, *Proc. Natl. Acad. Sci. U.S.A.* **93**, 5151 (1996); E. Diaz, F. Schimmöller, S. R. Pfeffer, *J. Cell Biol.* **138**, 283 (1997); Y. Wang, M. Okamoto, F. Schmitz, K. Hofmann, T. Südhof, *Nature* **388**, 593 (1997).
3. M. Sogaard *et al.*, *Cell* **78**, 937 (1994); P. Brenwald *et al.*, *ibid.* **79**, 245 (1994); J. P. Lian, S. Stone, Y. Jiang, P. Lyons, S. Ferro-Novick, *Nature* **372**, 698 (1994); L. Johannes *et al.*, *J. Cell Sci.* **109**, 2875 (1996); V. V. Lupashin and M. G. Waters, *Science* **276**, 1255 (1997).
4. F. Feiguin, A. Ferreira, K. S. Kosik, A. Caceres, *J. Cell Biol.* **127**, 1021 (1994); J. Lippincott-Schwartz, N. B. Cole, A. Marotta, P. A. Conrad, G. S. Bloom, *ibid.* **128**, 293 (1995); H. V. Goodson, C. Valetti, T. E. Kreis, *Curr. Opin. Cell Biol.* **9**, 18 (1997).
5. G. S. Bloom and S. A. Endow, *Protein Profile* **2**, 1105 (1995).
6. B. Goud, A. Zahraoui, A. Tavitian, J. Saraste, *Nature* **345**, 553 (1990); O. Martinez *et al.*, *J. Cell Biol.* **127**, 1575 (1994); O. Martinez *et al.*, *Proc. Natl. Acad. Sci. U.S.A.* **94**, 1828 (1997); O. Martinez, thesis, University of Paris, 1997.
7. Single-letter abbreviations for the amino acid residues are as follows: A, Ala; C, Cys; D, Asp; E, Glu; F, Phe; G, Gly; H, His; I, Ile; K, Lys; L, Leu; M, Met; N, Asn; P, Pro; Q, Gln; R, Arg; S, Ser; T, Thr; V, Val; W, Trp; X, any amino acid; and Y, Tyr.
8. The yeast reporter strain L40, which contains the reporter genes *lacZ* and *HIS3* downstream of the binding sequences for LexA, was sequentially transformed with the pLexA-Rab6 Q72L plasmid and with a mouse embryo randomly primed cDNA library in the pVP16 plasmid [A. B. Vojtek, S. M. Hollenberg, J. A. Cooper, *Cell* **74**, 205 (1993)]. The double transformants were plated on synthetic medium lacking histidine, leucine, tryptophan, uracil, and lysine and grown for 3 days at 30°C. His⁺ colonies were patched on selective plates and assayed for β -galactosidase activity. Library plasmids were rescued from His⁺-LacZ⁺ colonies and further analyzed by cotransformation tests and DNA sequencing.

pLexA-Rab6, pLexA-Rab6 Q72L, pLexA-Rab6 N126I, pLexA-Rab6 T27N, and pLexA-Rab6 Q22V have been previously described [I. Janoueix-Lerousey, F. Jollivet, J. Camonis, P. N. Marche, B. Goud, *J. Biol. Chem.* **270**, 14801 (1995)]. pLexA-Rab6 Q72L,I46E was obtained by cloning from pGEM-1-Rab6 Q72L,I46E (L. Johannes *et al.*, manuscript in preparation).

9. A. Echard *et al.*, data not shown.
10. An oligo deoxyribosylthymine and randomly primed cDNA λ gt10 library from adult BALB/c mouse testis (Clontech, Palo Alto, CA) was screened with the ³²P-labeled 174 cDNA fragment isolated by the two-hybrid screen. Four partially overlapping phages were first isolated out of 500,000 independent clones. We then screened 10⁶ phages with a fragment corresponding to the most 5' end of one of the previously isolated clones. Among the four overlapping clones isolated, one was found to contain the complete sequence presented in Fig. 1B. Phage inserts were subcloned in the pBSKS vector and sequenced with the Sanger dideoxy-termination method. Sequence analysis was performed with the GCG Wisconsin (Genetics Computer Group, Madison, WI) software package.
11. J. T. Yang, R. A. Laymon, L. S. Goldstein, *Cell* **56**, 879 (1989); J. T. Yang, W. M. Saxton, R. J. Stewart, E. C. Raff, L. S. B. Goldstein, *Science* **249**, 42 (1990).
12. The BL21(DE3) *Escherichia coli* strain was transformed with the pET15b (Novagen, Madison, WI) expression vector containing either his-tagged predicted motor domain (Nt, residues 1 to 530) or his-tagged stalk plus tail domains (Ct, residues 529 to 887) of Rabkinesin-6. Induction was performed for 4 hours at 37°C with 0.3 mM isopropyl- β -D-thiogalactopyranoside. Purification was achieved by adsorption on nickel beads under native conditions for Nt or denaturing conditions followed by renaturation steps for Ct (QIAexpressionist, QIAGEN). Purified his-tagged Nt and Ct were then dialyzed against 15 mM imidazole (pH 7), 2 mM MgCl₂, 1 mM EGTA, and 1 mM dithiothreitol or 80 mM KOH-Pipes (pH 6.9), 1 mM MgCl₂, and 1 mM EGTA, respectively. Protein concentrations were estimated by the Bradford assay.
13. Tubulin was purified from bovine brain with two cycles of polymerization followed by chromatography on phosphocellulose essentially as described [R. C. Williams and J. C. Lee, *Methods Enzymol.* **85**, 376 (1982)]. Microtubules (1 mg/ml) were polymerized with 20 μ M taxol. Microtubule concentration was expressed per tubulin heterodimer. Microtubule-binding assays were performed by incubating for 20 min at 33°C purified his-tagged Nt or Ct with taxol-stabilized MTs (ratio 1.5:1 or 1:1, respectively) in binding buffer [80 mM KOH-Pipes (pH 6.9), 1 mM MgCl₂, 1 mM EGTA, 1 mM GTP, and 20 μ M taxol]. The samples were then centrifuged in a TLX100 (Beckman, Palo Alto, CA) ultracentrifuge (TLS 55 rotor, 100,000g, 20 min, 33°C) on a 15% sucrose cushion. The release of Nt was performed by incubating pellets containing Nt-MT complexes with 10 mM Mg-ATP in the binding buffer for 20 min at 33°C, followed by centrifugation under the conditions described above. Equal amounts of pellet and supernatant were analyzed by SDS-polyacrylamide gel electrophoresis (SDS-PAGE). Microtubule-activated ATPase rates were measured at 25°C by the reduced form of NAD⁺ (NADH) coupled enzymes procedure. His-tagged Nt (55 nM) and increasing concentrations of taxol-stabilized MT (0 to 1.1 μ M) were incubated in a reaction buffer consisting of 20 mM KOH-Pipes (pH 6.9), 5 mM MgCl₂, 1 mM phosphoenolpyruvate, 267 μ M β -NADH, lactate dehydrogenase (0.1 mg/ml), and pyruvate kinase (0.1 mg/ml) and supplemented with 1 mM Mg-ATP [the Michaelis constant for ATP in the presence of MTs was found to be 85 μ M (9)]. Basal ATPase activity was determined at 25°C in the same reaction buffer with increasing concentrations of his-tagged Nt (from 55 to 930 nM).
14. R. Kuriyama *et al.*, *J. Cell Sci.* **107**, 3485 (1994).
15. A polyclonal rabbit antiserum was raised to purified glutathione S-transferase-tagged 174 protein ex-

- pressed in *E. coli*. HeLa cells were mechanically broken with a barrel-type homogenizer. Total extract, postnuclear supernatant (PNS), high speed pellet, and supernatant were prepared in 50 mM Hepes (pH 7.1) and 90 mM KCl with protease inhibitors, resolved by SDS-PAGE, and immunoblotted essentially as described [M. Roa, V. Cornet, C. Z. Yang, B. Goud, *J. Cell Sci.* **106**, 789 (1993)].
16. HeLa cells were fixed in methanol for 4 min at -20°C and processed for confocal laser scanning microscopy and immunofluorescence analysis as described (6). Images were recorded and imported into Adobe Photoshop 4.0 for compilation.
 17. B. J. Jasmin, J. Cartaud, M. Bornens, J. P. Changeux, *Proc. Natl. Acad. Sci. U.S.A.* **86**, 7218 (1989).
 18. HeLa cells were transfected with pEGFP-Rabkinesin-6 for 18 hours, with the DOTAP reagent (Boehringer Mannheim). To obtain Rabkinesin-6 fused at its NH₂-terminus with GFP, we introduced the blunted Sma I-Hind III fragment from pGEM-Rabkinesin-6 into the Sma I-digested pEGFP-C1 plasmid (Clontech). pGEM-Rabkinesin-6 was obtained after the creation of a Sma I site upstream of the initiator methionine of Rabkinesin-6 cDNA by polymerase chain reaction amplification with the primers 5'-GAACCCGGGAATGTCTCACCGGATCCTT-3' and 5'-GGGAATTCGAAGGTAACCTTTC-3', followed by cloning into Sma I-Eco RI sites of the pGEM-4Z plasmid (Promega).
 19. N. Hirokawa *et al.*, *Cell* **56**, 867 (1989); D. A. Skoufias, D. G. Cole, K. P. Wedaman, J. M. Scholey, *J. Biol. Chem.* **269**, 1477 (1994).
 20. HeLa cells were transfected with pGEM-Nt or pGEM-Ct for 4 hours, with the vaccinia system (6). To obtain pGEM-Nt and pGEM-Ct, we first added the double-strand DNA linker 5'-CCCGGGAGC-CATGGTTCCTCAGGTTTGAGGTACCGAATTC-3' between the Sma I and Eco RI sites of the pGEM-4Z plasmid to create a Bsu 36I restriction site, a stop codon, and an initiation codon in an optimal Kozak's context (pGEM4Z*). pGEM-Nt was obtained by introducing the Sma I-Bsu 36I fragment from pGEM-Rabkinesin-6 into pGEM4Z*. pGEM-Ct was obtained by introducing the Bsu 36I digestion fragment of pGEM-Rabkinesin-6 into Bsu 36I-digested pGEM4Z*. pGEM-myc-Nt and pGEM-myc-Ct were constructed by ligating the double-strand DNA linker 5'-GCATGCCACCATGGAACA-AAAACATCTCTCAGAAGAGGATCTGAATGACCCGGG-3' (encoding for MEQKLISEEDLN) (7) into Sph I-Sma I-digested pGEM-Nt and pGEM-Ct plasmids, respectively.
 21. S. B. Andrews, P. E. Gallant, R. D. Leapman, B. J. Schnapp, T. S. Reese, *Proc. Natl. Acad. Sci. U.S.A.* **90**, 6503 (1993); R. Chandra, E. Salmon, H. Erickson, A. Lockart, S. Endow, *J. Biol. Chem.* **268**, 9005 (1993).
 22. pGEM-myc-Rabkinesin-6 was constructed by ligating the double-strand DNA linker 5'-GCATGCCAC-CATGGAACAAAACATCTCTCAGAAGAGGATCT-GAATGACCCGGG-3' (encoding for MEQKLISEEDLN) (7) into Sph I-Sma I-digested pGEM-Rabkinesin-6 plasmid. HeLa cells were cotransfected with the vaccinia system (6) with pGEM-myc-Rabkinesin-6, pGEM-myc-Nt (20), or pGEM-myc-Ct (20) plasmids (1.5 $\mu\text{g}/\text{well}$) and either pGEM-1 (control) or plasmids encoding for Rab6 constructs (6) (1.5 $\mu\text{g}/\text{well}$). After 4 hours, cells were incubated for 15 min in medium without methionine and cysteine (ICN Pharmaceuticals, Costa Mesa, CA) and metabolically labeled for 20 min with [³⁵S]methionine (250 $\mu\text{Ci}/\text{ml}$) and [³⁵S]cysteine (250 $\mu\text{Ci}/\text{ml}$) (Amersham). After a 30-min chase in complete medium supplemented with 2.5 mM methionine and cysteine, cells were lysed in 1% Nonidet P-40 (Sigma), 20 mM Hepes (pH 7.4), 150 mM NaCl, 5 mM MgCl₂, 0.2% bovine serum albumin, 1 mM phenylmethylsulfonyl fluoride, and a mixture of protease inhibitors by incubation at 4°C for 10 min. Supernatants obtained after centrifugation for 10 min at 20,000g were precleared by incubation with protein-G Sepharose for 30 min at 4°C. After preclearing, the supernatants were incubated with 9E10 anti-myc (and in one experiment with affinity-purified anti-Rab6) together with protein-G Sepharose beads for 1 hour at 4°C. The immunoprecipitates were then washed 4 times in the lysis buffer and analyzed by SDS-PAGE and autoradiography.
 23. Transport of SEAP was monitored essentially as described (6). Briefly, HeLa cells cotransfected with pGEM-SEAP and various constructs encoding plasmids were labeled for 4 hours with [³⁵S]methionine (50 $\mu\text{Ci}/\text{ml}$) and [³⁵S]cysteine (50 $\mu\text{Ci}/\text{ml}$). SEAP present in cell lysates or in the medium was immunoprecipitated with a polyclonal antibody to calf intestine alkaline phosphatase (Rockland). Immunoprecipitates were then digested with endoglycosidase H (endo H) (Sigma). Endo H treatment allowed us to distinguish two intracellular forms of SEAP: SEAP molecules bearing endo H-sensitive oligosaccharides still present in compartments before *cis*-medial Golgi (mainly ER) and endo H-resistant molecules (also sensitive to neuraminidase) corresponding to SEAP that have reached late Golgi-TGN compartments. Immunoprecipitates were then analyzed by SDS-PAGE and autoradiography. Bands corresponding to SEAP were quantified with a PhosphorImager (Molecular Dynamics) equipped with the Image Quant software.
 24. D. Deretic *et al.*, *J. Cell Sci.* **108**, 215 (1995); J. Peränen, P. Auvinen, H. Virta, R. Wepf, K. Simons, *J. Cell Biol.* **135**, 153 (1996).
 25. The conserved domains are RXRP (amino acids 69 to 72), YGQ(T/S)X(T/S/A)GK(T/S) (amino acids 158 to 166, except for the Q replaced by a V as in CHO1 or HMKLP1), NXXSSRSH (amino acids 373 to 380), and DLAGXE (amino acids 407 to 412) (7). Highly conserved residues EXYXE/DXXXDLL (amino acids 306 to 316) and (L/V)P(F/Y)R (amino acids 456 to 459), possibly corresponding to MT-binding sites, are also present [E. P. Sablin, F. J. Kull, R. Cooke, R. D. Vale, R. J. Fletterick, *Nature* **380**, 555 (1996)].
 26. A. Lupas, M. Van Dyke, J. Stock, *Science* **252**, 1162 (1991).
 27. We thank M. Bornens, M.-H. Cuif, B. Hoflack, L. Johannes, G. Langsley, J. de Mey, M. Kress, J.-L. Rigaud, J. Salamero, and C. Saudrais for critical reading of this manuscript and helpful discussions; M. Bornens (Institut Curie, Paris), E. Berger (Zurich, Switzerland), M. Zerial [European Molecular Biology Laboratory (EMBL), Heidelberg, Germany], and P. Chavrier (Centre d'Immunologie de Marseille-Luminy, Marseille, France) for the gifts of CTR 433 monoclonal antibody, affinity-purified polyclonal antibody to human β -1,4-galactosyltransferase, pLexA-Rab5 Q79L, and pLexA-Rab7 Q67L, respectively; and G. Bordenave for help in rabbit immunization. Supported in part by grants from the Association de la Recherche Contre le Cancer, the Fondation de la Recherche Médicale, the European Community, and the Human Frontier Science Program.

2 October 1997; accepted 2 December 1997

Location, Location, Location...

Discover SCIENCE Online and take advantage of these features...

- Fully searchable database of abstracts and news summaries for current & past SCIENCE issues
- Interactive projects, special features and additional data found in the Beyond the Printed Page section
- SCIENCE Professional Network & Electronic Marketplace

Tap into the sequence below and see SCIENCE Online for yourself.

www.sciencemag.org

SCIENCE